

A primary study on biological behavior of aluminum using ^{26}Al -AMS

Song-Mei Qin^{1,2} · Xiang-Gao Wang^{2,3} · Xiao-Xi Lan^{2,3} · Yun-Ting Gu^{2,3} ·
Ke-Jun Dong⁴ · Ming He⁴ · Shan Jiang⁴

Received: 13 April 2015 / Revised: 27 August 2015 / Accepted: 28 September 2015 / Published online: 6 May 2016
© Shanghai Institute of Applied Physics, Chinese Academy of Sciences, Chinese Nuclear Society, Science Press China and Springer Science+Business Media Singapore 2016

Abstract Aluminum is concerned as a possible cause of many diseases. To investigate the long-term Al biokinetics and bioavailability in various kinds of Al-contained medicine and food, an accelerator mass spectrometry (AMS) based on the HI-13 tandem has been established for biological analysis with ^{26}Al ($T_{1/2} = 716,000$ years) as the tracer. In this paper, the animal tracing, sample preparation procedure and ^{26}Al -AMS measurement are presented. The sample preparation procedure has been simplified. A high sensitivity of 5×10^{-15} for $^{26}\text{Al}/^{27}\text{Al}$ has been achieved. Two phases were found before and after a break time (t_b) for the ^{26}Al retained in blood and brain, with $t_b \approx 8$ and 12 h after the ^{26}Al tracer injection, respectively.

Keywords ^{26}Al · Accelerator mass spectrometry · Biological tracing

This study was supported by National Natural Science Foundation of China (No. 41166002), Guangxi Natural Science Foundation (Nos. 2012GXNSFBA053004, 2013GXNSFFA019001) and Guangxi New Century Education Project (No. 2013JGZ100).

✉ Xiang-Gao Wang
wangxg@gxu.edu.cn

¹ Guangxi University of Chinese Medicine, Nanning 530001, China

² GXU-NAOC Center for Astrophysics and Space Sciences, Department of Physics, Guangxi University, Nanning 530004, China

³ Guangxi Key Laboratory for the Relativistic Astrophysics, Nanning 530004, China

⁴ China Institute of Atomic Energy, Beijing 102413, China

1 Introduction

Aluminum is the most abundant metal element in the environment and is the most common metal element in our life. It is also a trace element in human body, but not the essential one. In medicine, chemical Al-compounds are used as antiseptic, alum, antacid or phosphate binder for dialysis patients with renal failure. On the other hand, Al is concerned as a cause of many diseases (e.g., osteopathy, anemia and encephalopathy) [1–5], if its intake is too much.

As shown in Table 1, neither of the radioisotopes is suitable for use as a tracer to study Al biological behavior and bioavailability in animals and human, which had been carried out by employing just the stable isotope ^{27}Al [3] before 1990. Since the natural level of ^{27}Al in the environment (~ 0.1 g/g) is far greater than that in biological samples (10^{-6} – 10^{-8} g/g), the research on behaviors of Al in animals and human had been obstructed by difficulties in distinguishing the trace amount of Al in biological samples from the environment.

Therefore, two tracer approaches are well accepted to study Al biokinetics. One is the use of congeners, such as radioactive ^{67}Ga , based on similar chemical properties of Al and Ga. However, their chemical reactions in body are different [6, 7]. Another one is the accelerator mass spectrometry (AMS) [8–13], or ultra-sensitivity mass spectrometry, using ^{26}Al , the only long-life radioisotope of Al ($T_{1/2} = 716,000$ years), and the only Al isotope being capable of tracing research, but quite difficult, though. The methods for measuring ^{26}Al include decay counting and conventional mass spectrometry (MS). MS cannot discriminate ^{26}Al from the ^{26}Mg isobar, while the decay counting method to detect the trace amount of ^{26}Al (close

Table 1 The information of isotopes of aluminum

Isotopes	^{25}Al	^{26}Al	^{27}Al	^{28}Al	^{29}Al
$T_{1/2}$	7.2 s	716,000 years	Stable	2.3 min	6.6 min

to detection limits) is of large uncertainties. Therefore, ^{26}Al tracer in medical application is very difficult without AMS, which advantages over MS methods in its high sensitivity, small sample size requirement, free from isobar and molecular ion interferences, and short measurement time.

Taking advantages of nonmeasurable ^{26}Al in the environment or in normal biological organisms, the ^{26}Al -AMS approach, which avoids interference of endogenous Al in studying Al biokinetic and bioavailability, has been carried out in several groups [2, 3, 14–25]. Studies with ^{26}Al -AMS on mice aluminum biokinetic were performed by the groups in Manchester [3, 15, 16], Orsay [17], Zurich [18], Tokyo [19], Munich-Aachen [2] and Kentucky [20]. The Manchester and Munich-Aachen groups did studies on human Al biokinetic, too. They found that some Al is retained in the body, most probably within the skeleton and brain. Most of Al that enters the blood is excreted in urine within a few days or weeks. Al bioavailability was estimated in a number of ^{26}Al -AMS studies, including a model food and biscuit containing acidic SALP [20–24]. It was also found that typical human foods have high Al bioavailability, but still, there are Al-contained medicine and food with unknown Al biokinetic and bioavailability. Too much human intake of Al may be retained in skeleton and brain, which may cause osteopathy, anemia and encephalopathy.

We need ^{26}Al -AMS to investigate the long-term Al biokinetics and bioavailability in Al-contained medicine and food in China. In this paper, a ^{26}Al -AMS tracing method is established and the primary results are presented.

2 Materials and methods

2.1 Animals

Wistar rats of 2-month old were purchased from Guangxi Medical University, Nanning, China, and fed with standard diet. All animal experiments were performed according to the Guidelines for the Care and Use of Laboratory Animals [26]. The mice were divided into the experimental, control and background groups, with three mice in each group. The tracer isotope ^{26}Al is the laboratory standard kept from 1996 at the AMS lab of China Institute of Atomic Energy (CIAE) AMS. Decay counting method was used to calibrate the $^{26}\text{Al}/^{27}\text{Al}$ ratio. The $^{26}\text{Al}/^{27}\text{Al}$ ratio of AlCl_3 solution for injection was

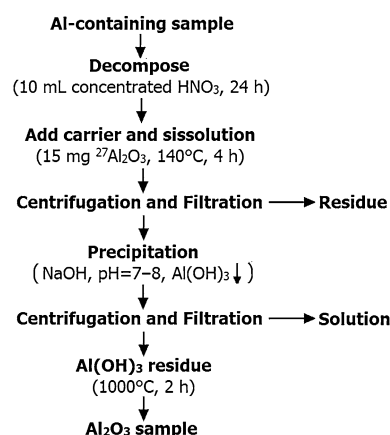
1.5×10^{-9} , with the ^{26}Al content of $2.5 \mu\text{g/mL}$. The solution was prepared by successive dilution of the original standard sample. The three animal groups were treated as follows:

1. *Experimental group* The mice are used to inject ^{26}Al for experimental tracing. Thirty mice were divided into 10 subgroups ($n = 3$) for 10 timescales. The mice were tail mainline injected with 1 mL of $^{26}\text{AlCl}_3$ (pH 4.5) and were blood-sampled and euthanized for brain sampling at 0.5, 2, 4, 8, 16, 48, 72, 96, 120 and 168 h after injection.
2. *Control group* ($n = 3$) The mice were injected with 1 mL $^{27}\text{AlCl}_3$ solution, for the behavior observation.
3. *Background group* ($n = 3$) The mice were injected with 1 mL normal saline solution for AMS measurement of the ^{26}Al as background sample.

2.2 Sample preparation

The beam current of $^{26}\text{AlO}^-$ is 20–40 times higher than the $^{26}\text{Al}^-$, but the number of ^{26}Mg isobar will become too large to identify ^{26}Al of ultra-low level. Besides, the particle transmission of single atom is higher than molecular ions. Therefore, a single atomic negative Al^- form is adopted in our AMS measurement. Taking advantage of the electric potential of Mg electron affinity is lower than zero, Mg^- ions cannot be extracted, but the Al^- can, from the AMS multi-cathode source. As the interfere isobar ^{26}Mg is no longer a problem, a simplified preparation process was developed (Fig. 1).

1. The blood/brain samples were decomposed with 10 mL of concentrated nitric acid at 80°C for 24 h in a Teflon-sealed vessel.

**Fig. 1** Sample preparation procedure

- After cooling, 15 mg of $^{27}\text{AlCl}_3$ was added in the sample solution as a carrier and then heated at 140 °C for 4 h in a Teflon-sealed vessel inserted in a stainless steel bottle.
- After cooling, the blood samples were centrifuged and Al-contained solution samples will be obtained.
- Add NaOH solution to the Al-containing sample solution and carefully adjust the solution to pH 7–8. $\text{Al}(\text{OH})_3$ sediment can be formed at pH 7–8, while a very few of $\text{Mg}(\text{OH})_2$ can be formed at this pH value. Therefore, the most of ^{26}Mg , isobar of our interesting isotope ^{26}Al could be eliminated in this step.
- $\text{Al}(\text{OH})_3$ sediment was obtained via centrifugation and then converted to Al_2O_3 at 1000 °C for 2 h.

In the AMS measurement, each sample was mixed with an equal mass of pure silver powder for improving thermal and electric conductivity and pressed into a sample holder of a 40-sample NEC MC-SNICS ion source.

2.3 Analysis of ^{26}Al by accelerator mass spectrometry

The number of ^{26}Al was measured with the AMS at CIAE (Fig. 2). Since its installation in 1989, ^{26}Al , ^{36}Cl , ^{41}Ca , ^{55}Fe , ^{64}Gu , ^{79}Se , ^{99}Tc , ^{129}I , ^{151}Sm , ^{182}Hf , ^{236}U and ^{237}Np have been measured for applications in biomedicine, nuclear physics, nuclear astrophysics and environmental science [11, 27–36]. Figure 2 shows schematically the AMS system based on an HI-13 Tandem accelerator. This work was carried out on AMS beamline 1. The AMS beamline 2 was for AMS research of medium-heavy mass nuclides.

Single atomic ions of Al^- from the ion source are selected by the low-energy magnetic analysis system for injection into HI-13 Tandem accelerator, typically with

40 nA beam current at the lower-energy Faraday cup (LEFC). The Al^- ions are pre-accelerated to 110 keV in the low-energy system and to 7 MeV by the first column of the tandem accelerator. The negative ions are stripped by a 3- $\mu\text{g}/\text{cm}^2$ -thick carbon foil, and the position ions are further accelerated in the second column by the terminal voltage. A 90° double-focusing analyzing magnet was used to select ions $^{26}\text{Al}^{7+}$, with energy of 56.1 MeV. According to theoretical simulation of the charge stripping, the charge state 7+ at 7 MV has a large fraction of ~34 %. The $^{26}\text{Al}^{7+}$ ion beams are transported to the AMS Beamline 1 and detection system, with a switching magnet and 15° electrostatic deflector. The analyzer magnet, switching magnet, electrostatic analyzer and other beam optical elements are adjusted to obtain optimal $^{26}\text{Al}^{7+}$ beam line.

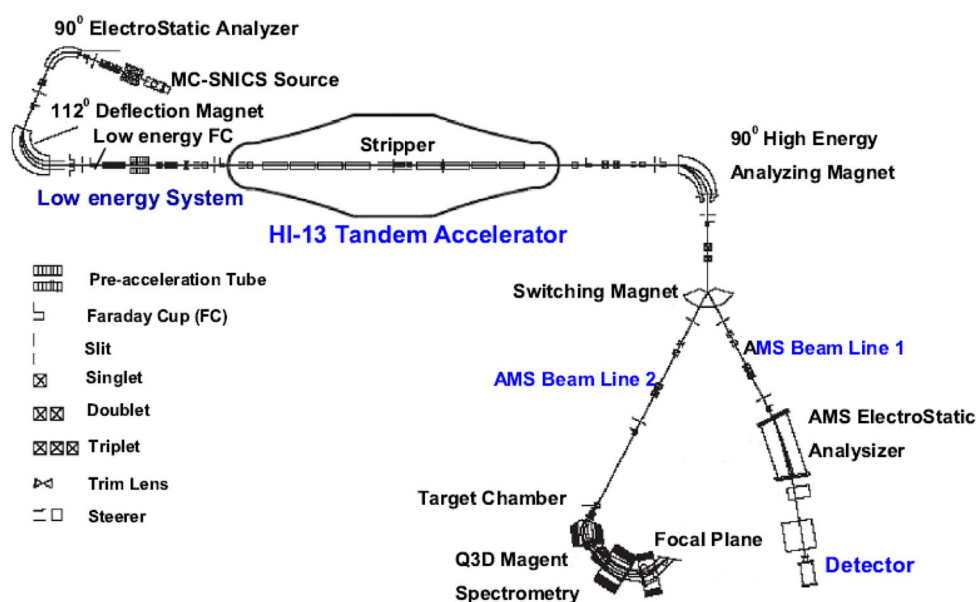
Since no interference of ^{26}Mg isobar, a Si(Au) surface barrier detector is used to record the number and energy of the $^{26}\text{Al}^{7+}$. The ^{27}Al beam current is record by the LEFC in low-energy system, and the $^{26}\text{Al}/^{27}\text{Al}$ isotope ratios can be obtained. In this study, each sample was measured at least three times. All isotope ratios were normalized by $^{26}\text{Al}/^{27}\text{Al}$ standards sample.

3 Results

3.1 ^{26}Al -AMS based on extracting Al^- ions

Typically, the beam current of $^{27}\text{Al}^-$ is ~40 nA at LEFC. The ions extracting is stable (Fig. 3), which is crucial for measurement precision. Typical current is lower than that at UTTAC and SUERC [37, 38], because of mainly the low electron affinity of Al, and the not-so-good

Fig. 2 Schematic diagram of the accelerator mass spectrometer based on the HI-13 tandem accelerator at CIAE



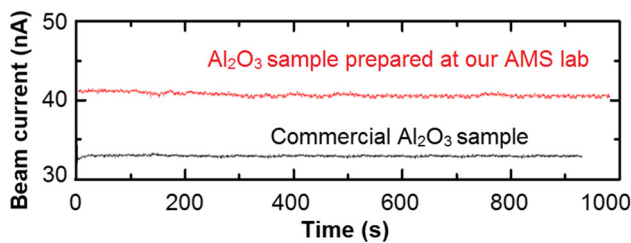


Fig. 3 Beam currents of $^{27}\text{Al}^-$ of the commercial Al_2O_3 sample and biological Al_2O_3 sample prepared at our AMS lab

ion source and low-energy system, caused by a low vacuum problem at that time. However, this did not have much effect on this work.

The preparation of biological sample is a key step in the tracing experiment. As shown in Fig. 3, beam current of the prepared Al_2O_3 sample is over 40 nA, and it is larger than that of commercial sample. The overall particle transmission between the low-energy injection system and the detection system is $\sim 3\%$. Figure 4a is the 56.1 MeV $^{26}\text{Al}^{7+}$ ion spectra of the background sample prepared with the same sample preparation procedure. It demonstrates that there were no interference isotopes in our measurement. The combination of our sample preparation procedure and extraction of single atomic negative Al^- from the ion source, the ^{26}Mg isobar, is highly suppressed. Figure 4b is spectra of the blood sample, and it can be sure that the peak at 56.1 MeV is the counts of $^{26}\text{Al}^{7+}$ ions. The simplicity preparation procedure can satisfy the biological tracing requirement.

We used the blank sample (commercial Al_2O_3 and our background sample) to test the AMS system. The sensitivity is good, with the $^{26}\text{Al}/^{27}\text{Al}$ ratio of lower than 5×10^{-15} .

3.2 Al biological behavior in blood

In this work to establish the ^{26}Al -AMS method for biological tracing, the $^{26}\text{Al}/^{27}\text{Al}$ ratio, instead of the ^{26}Al concentration, is used. The ^{26}Al concentration can be obtained from $^{26}\text{Al} = (^{26}\text{Al}/^{27}\text{Al}) \text{ ratio} \times ^{27}\text{Al}$ concentration, which can be measured by spectrophotometry.

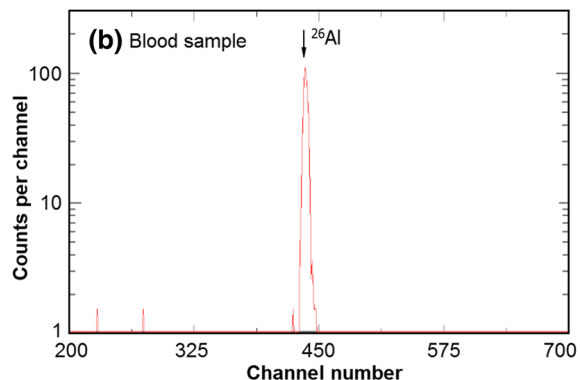
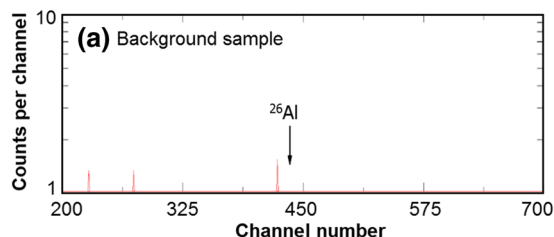


Fig. 4 Spectra of 56.1 MeV $^{26}\text{Al}^{7+}$ ions, detected by a Si(Au) surface barrier detector

The data of $^{26}\text{Al}/^{27}\text{Al}$ ratios in blood are shown in Fig. 5. Because of limit in beam time of the tandem accelerator, we measured the blood samples of six time points (0.5, 2, 8, 16, 48, 168 h). The data could be fitted with a nonlinear function:

$$^{26}\text{Al}/^{27}\text{Al} = 1.63 \times 10^{-10} t^{-(1.588 \pm 0.355)}.$$

The decrease index is similar with the result of Priest et al. [3], who found that the Al concentration (A_{Al}) in the blood after injection varied in a function of time as $A_{\text{Al}} = 0.206 t^{-1.250}$.

We also found, as shown in Fig. 5, that the data also can be well fitted by a two-component function of time,

$$^{26}\text{Al}/^{27}\text{Al} = 1.85 \times 10^{-11} \left[(t/t_b)^{-(0.457 \pm 0.121)} + (t/t_b)^{-(2.921 \pm 0.195)} \right],$$

where the $t_b \approx 8$ h is break time and the exponents $-(0.457 \pm 0.121)$ and $-(2.921 \pm 0.195)$ denote, respectively, the time before and after t_b , corresponding to the slow and fast decrease phase.

3.3 Al biological behavior in brain

Brain samples of five time points (2, 16, 48, 72 and 168 h) were measured. The $^{26}\text{Al}/^{27}\text{Al}$ results are shown in Fig. 6. It can be seen that the brain $^{26}\text{Al}/^{27}\text{Al}$ ratio went up quickly in 16 h after the Al injection. It retained stable in the first week, with a nonlinear function of $^{26}\text{Al}/^{27}\text{Al} = 1.41 \times 10^{-13} t^{-(0.142 \pm 0.136)}$.

Also, the data could be well fitted by a two-component function of time, as shown in Fig. 6,

$$^{26}\text{Al}/^{27}\text{Al} = 1.10 \times 10^{-13} \left[(t/t_b)^{(1.620 \pm 0.125)} + (t/t_b)^{-(0.142 \pm 0.136)} \right],$$

where the $t_b \approx 12$ h is the break time. The Al content in brain increased before t_b with an increase index of 1.620 ± 0.125 , corresponding to the slow decrease phase of the blood sample (Fig. 5). After the Al came into the

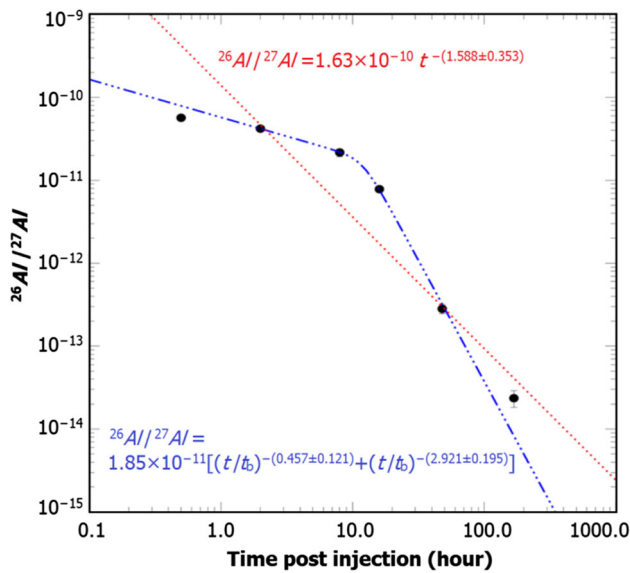


Fig. 5 Biological behavior of $^{26}\text{Al}/^{27}\text{Al}$ in blood. The data are fitted by a nonlinear function and a two-component function ($t_b \approx 8$ h)

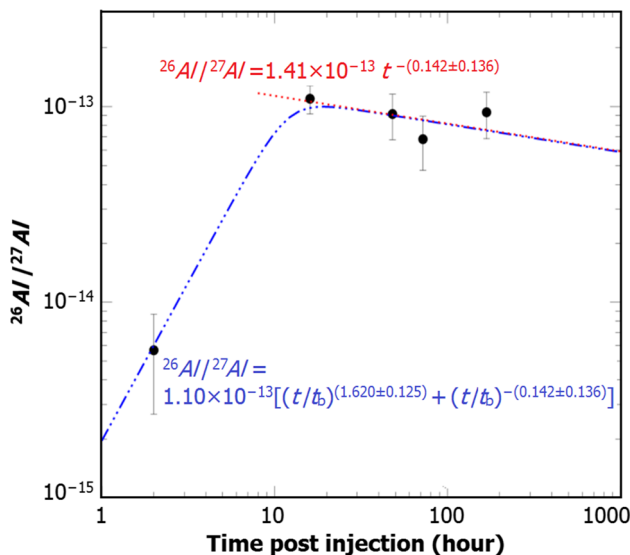


Fig. 6 Biological behavior of $^{26}\text{Al}/^{27}\text{Al}$ in brain. The data are fitted by a nonlinear function and a two-component function ($t_b \approx 12$ h)

brain, it would decrease slowly, with a decrease index of $-(0.142 \pm 0.136)$. If the Al intake continues, the Al accumulated in brain would cause many kinds of diseases.

4 Conclusion

In conclusion, a ^{26}Al -AMS tracing method including the animal tracing, sample preparation and AMS measurement have been established on the HI-13 tandem accelerator. The sample preparation procedure is simplified and easy to

achieve. By extracted single atomic negative Al^- from ion source, taking advantage of the lack of any isobaric interference, a high sensitivity of lower than 5×10^{-15} for $^{26}\text{Al}/^{27}\text{Al}$ has been achieved.

We found that the $^{26}\text{Al}/^{27}\text{Al}$ ratio in blood and brain behaved as a two-component function of time. The blood $^{26}\text{Al}/^{27}\text{Al}$ ratios show a low and a fast decrease phase before and after a break time t_b (about 8 h post-injection), with a decrease index $-(0.457 \pm 0.121)$ and $-(2.921 \pm 0.195)$, respectively. These two phases are related to the fast increase and slow decrease phase in the brain $^{26}\text{Al}/^{27}\text{Al}$ ratios, before and after a time t_b time (about 12 h post-injection), with the index (1.620 ± 0.125) and $-(0.142 \pm 0.136)$. After the time t_b , the Al in the brain decreased very slowly. If the Al intake continues, the Al accumulation in the brain will cause many kinds of diseases.

Further experiments are needed to prove the Al biological behavior.

Acknowledgments We thank Prof. Zou-Wen Zheng from Guangxi University of Chinese Medicine for the help in the animal tracing experiments.

References

1. A.C. Alfrey, G.R. LeGendre, W.D. Kaehny, The dialysis encephalopathy syndrome—possible aluminum intoxication. *N. Engl. J. Med.* **294**, 184–188 (1976). doi:[10.1056/NEJM197601222940402](https://doi.org/10.1056/NEJM197601222940402)
2. Ch. Hohl, P. Gerisch, G. Korschinek et al., Medical application of ^{26}Al . *Nucl. Instrum. Methods B* **92**, 478–482 (1994). doi:[10.1016/0168-583X\(94\)96058-5](https://doi.org/10.1016/0168-583X(94)96058-5)
3. N.D. Priest, The biological behaviour and bioavailability of aluminium in man, with special reference to studies employing aluminium-26 as a tracer: review and study update. *J. Environ. Monitor.* **6**, 375–403 (2004). doi:[10.1039/B314329P](https://doi.org/10.1039/B314329P)
4. M. Kawahara, Effects of aluminum on the nervous system and its possible link with neurodegenerative diseases. *J. Alzheimers Dis.* **8**, 171–182 (2005)
5. WHO, *Background Document for Development of WHO Guidelines for Drinking-Water Quality*, 4th edn. http://www.who.int/water_sanitation_health/publications/dwq_guidelines/en/
6. N.D. Priest, D. Newton, J.P. Day et al., Human metabolism of aluminium-26 and gallium-67 injected as citrates. *Hum. Exp. Toxicol.* **14**, 287–293 (1995). doi:[10.1177/096032719501400309](https://doi.org/10.1177/096032719501400309)
7. C.B. Dobson, J.P. Day, S.J. King et al., Location of aluminium and gallium in human neuroblastoma cells treated with metal-chelating agent complexes. *Toxicol. Appl. Pharm.* **152**, 145–152 (1998). doi:[10.1006/taap.1998.8489](https://doi.org/10.1006/taap.1998.8489)
8. L.W. Alvarez, R. Cornog, He^3 in helium. *Phys. Rev.* **56**, 379 (1939). doi:[10.1103/PhysRev.56.379.2](https://doi.org/10.1103/PhysRev.56.379.2)
9. E.D. Nelson, R.G. Korteling, W.R. Stott, Carbon-14: direct detection at natural concentrations. *Science* **198**, 507–508 (1977). doi:[10.1126/science.198.4316.507](https://doi.org/10.1126/science.198.4316.507)
10. C.L. Bennett, R.P. Beukens, M.R. Clover et al., Radiocarbon dating using electrostatic accelerators: negative ions provide the key. *Science* **198**, 508–510 (1977). doi:[10.1126/science.198.4316.508](https://doi.org/10.1126/science.198.4316.508)

11. S. Jiang, M. He, S.S. Jiang et al., Development of AMS measurements and applications at the CIAE. Nucl. Instrum. Methods B **172**, 87–90 (2000). doi:[10.1016/S0168-583X\(00\)00370-0](https://doi.org/10.1016/S0168-583X(00)00370-0)
12. C.D. Shen, W.X. Yi, K.F. Yu et al., Holocene megathermal abrupt environmental changes derived from ^{14}C dating of a coral reef at Leizhou Peninsula, South China Sea. Nucl. Instrum. Methods B **B223–224**, 416–419 (2004). doi:[10.1016/j.nimb.2004.04.079](https://doi.org/10.1016/j.nimb.2004.04.079)
13. L. Liu, W.J. Zhou, P. Cheng et al., A new dual injection system for AMS facility. Nucl. Instrum. Methods B **259**, 208–212 (2007). doi:[10.1016/j.nimb.2007.01.160](https://doi.org/10.1016/j.nimb.2007.01.160)
14. S.L. Wang, Y.H. Liu, D.M. Li et al., Study of ^{26}Al measurement on the Shanghai Mini-cyclotron based AMS. Nucl. Instrum. Methods B **266**, 3302–3308 (2008). doi:[10.1016/j.nimb.2008.04.007](https://doi.org/10.1016/j.nimb.2008.04.007)
15. J.P. Day, J. Barker, S.J. King et al., Biological chemistry of aluminium studied using ^{26}Al and accelerator mass spectrometry. Nucl. Instrum. Methods B **92**, 463–468 (1994). doi:[10.1016/0168-583X\(94\)96055-0](https://doi.org/10.1016/0168-583X(94)96055-0)
16. J. Barker, J. Templar, S.J. King et al., AMS measurements to study uptake and distribution of ^{26}Al in mice and the role of the transferrin receptor in aluminium absorption mechanisms. Nucl. Instrum. Methods B **123**, 275–278 (1997). doi:[10.1016/S0168-583X\(96\)00704-5](https://doi.org/10.1016/S0168-583X(96)00704-5)
17. P. Jouhanneau, G.M. Raisbeck, F. Yiou et al., Gastrointestinal absorption, tissue retention, and urinary excretion of dietary aluminium in rats determined by using ^{26}Al . Clin. Chem. **43**, 1023–1028 (1997)
18. K.W. Schonholzer, R.A. Sutton, V.R. Walker, Intestinal absorption of trace amounts of aluminium in rats studied with ^{26}Al and accelerator mass spectrometry. Clin. Sci. **92**, 379–383 (1997). doi:[10.1042/cs0920379](https://doi.org/10.1042/cs0920379)
19. S. Yumoto, H. Nagai, M. Imamura et al., ^{26}Al uptake and accumulation in the rat brain. Nucl. Instrum. Methods B **123**, 279–282 (1997). doi:[10.1016/S0168-583X\(96\)00429-6](https://doi.org/10.1016/S0168-583X(96)00429-6)
20. B.H. Wang, G.S. Jackson, R.A. Yokel et al., Applying accelerator mass spectrometry for low-level detection of complex engineered nanoparticles in biological media. J. Pharm. Biomed. Anal. **294**, 39–42 (2014). doi:[10.1016/j.jpba.2014.04.003](https://doi.org/10.1016/j.jpba.2014.04.003)
21. R.A. Yokel, R.L. Florence, Aluminum bioavailability from tea infusion. Food Chem. Toxicol. **46**, 3659–3663 (2008). doi:[10.1016/j.fct.2008.09.041](https://doi.org/10.1016/j.fct.2008.09.041)
22. Y.Z. Zhou, W.R. Harris, R.A. Yokel, The influence of citrate, maltolate and fluoride on the gastrointestinal absorption of aluminium at a drinking water-relevant concentration: a ^{26}Al and ^{14}C study. J. Inorg. Biochem. **102**, 798–808 (2008). doi:[10.1016/j.jinorgbio.2007.11.019](https://doi.org/10.1016/j.jinorgbio.2007.11.019)
23. C. Steinhausena, G. Kislingera, C. Winkelhofera et al., Investigation of the aluminium biokinetics in humans: a ^{26}Al tracer study. Food Chem. Toxicol. **42**, 363–371 (2004). doi:[10.1016/j.fct.2003.09.010](https://doi.org/10.1016/j.fct.2003.09.010)
24. S. Yumoto, H. Nagai, S. Kakimi et al., ^{26}Al incorporation into the brain of rat fetuses through the placental barrier and subsequent metabolism in postnatal development. Nucl. Instrum. Methods B **268**, 1328–1330 (2010). doi:[10.1016/j.nimb.2009.10.165](https://doi.org/10.1016/j.nimb.2009.10.165)
25. C.H. Guo, Y.F. Lu, G.S. Wang, The influence of aluminum exposure on male reproduction and offspring in mice. Environ. Toxicol. Pharm. **20**, 135–141 (2005). doi:[10.1016/j.etap.2004.11.007](https://doi.org/10.1016/j.etap.2004.11.007)
26. National Research Council (US) Committee, *Guide for the Care and Use of Laboratory Animals*, 8th edn. (National Academies Press, Washington, DC, 2011)
27. M. He, S. Jiang, S.S. Jiang et al., Measurement of ^{79}Se and ^{64}Cu with PXAMS. Nucl. Instrum. Methods B **172**, 177–181 (2000). doi:[10.1016/S0168-583X\(00\)00393-1](https://doi.org/10.1016/S0168-583X(00)00393-1)
28. Y.J. Guang, M. He, X.D. Ruang et al., The development of a gas-filled time-of-flight detector. Nucl. Instrum. Methods B **259**, 213–216 (2007). doi:[10.1016/j.nimb.2007.01.310](https://doi.org/10.1016/j.nimb.2007.01.310)
29. K.J. Dong, M. He, S. Jiang et al., Measurement of trace ^{129}I concentrations in CsI powder and organic liquid scintillator with accelerator mass spectrometry. Nucl. Instrum. Methods B **259**, 271–276 (2007). doi:[10.1016/j.nimb.2007.01.232](https://doi.org/10.1016/j.nimb.2007.01.232)
30. X.G. Wang, S. Jiang, M. He et al., ^{236}U measurement with accelerator mass spectrometry at CIAE. Nucl. Instrum. Methods B **34**, 2295–2299 (2010). doi:[10.1016/j.nimb.2010.03.017](https://doi.org/10.1016/j.nimb.2010.03.017)
31. X.G. Wang, S. Jiang, M. He et al., Accurate determination of cross-sections for ^{238}U (n, 2n) ^{237}U induced by neutrons around 14 MeV. Nucl. Instrum. Methods A **621**, 326–330 (2010). doi:[10.1016/j.nima.2010.04.034](https://doi.org/10.1016/j.nima.2010.04.034)
32. X.Y. Yin, M. He, K.J. Dong et al., Measurement of ^{151}Sm with the HI-13 accelerator mass spectrometry system. Nucl. Instrum. Methods B **268**, 1689–1691 (2010). doi:[10.1016/j.nimb.2010.02.126](https://doi.org/10.1016/j.nimb.2010.02.126)
33. X.G. Wang, S. Jiang, K.J. Dong et al., Development of laboratory standards for AMS measurement of ^{237}Np . Nucl. Instrum. Methods B **268**, 1949–1953 (2010). doi:[10.1016/j.nimb.2010.02.106](https://doi.org/10.1016/j.nimb.2010.02.106)
34. K.J. Dong, L.Y. Lu, M. He et al., Study on bone resorption behavior of osteoclast under drug effect using ^{41}Ca tracing. Nucl. Instrum. Methods B **294**, 671–674 (2013). doi:[10.1016/j.nimb.2012.08.051](https://doi.org/10.1016/j.nimb.2012.08.051)
35. S. Jiang, M. He, K.J. Dong et al., Large projects at the accelerator mass spectrometry facility at the China Institute of Atomic Energy during the last 12 years. Nucl. Instrum. Methods B **294**, 39–42 (2013). doi:[10.1016/j.nimb.2012.02.011](https://doi.org/10.1016/j.nimb.2012.02.011)
36. X.G. Wang, S. Jiang, M. He et al., Determination of cross sections for the $^{238}\text{U}(n,3n)^{236}\text{U}$ reaction induced by 14-MeV neutrons with accelerator mass spectrometry. Phys. Rev. C **87**, 014612 (2013). doi:[10.1103/PhysRevC.87.014612](https://doi.org/10.1103/PhysRevC.87.014612)
37. K. Sasa, Y. Nagashima, T. Takahashi et al., ^{26}Al and ^{36}Cl AMS system at the University of Tsukuba: a progress report. Nucl. Instrum. Methods B **259**, 41–46 (2007). doi:[10.1016/j.nimb.2007.01.313](https://doi.org/10.1016/j.nimb.2007.01.313)
38. S. Xu, S.P. Freeman, D.H. Rood et al., Decadal ^{10}Be , ^{26}Al and ^{36}Cl QA measurements on the SUERC 5 MV accelerator mass spectrometer. Nucl. Instrum. Methods B **361**, 39–42 (2015). doi:[10.1016/j.nimb.2015.03.064](https://doi.org/10.1016/j.nimb.2015.03.064)